STRUCTURAL
BIOLOGY

Volume 78 (2022)

Supporting information for article:

Comparative study of the effects of high hydrostatic pressure *per se* and high argon pressure on urate oxidase ligand stabilization

Thierry Prangé, Philippe Carpentier, Anne-Claire Dhaussy, Peter van der Linden, Eric Girard and Nathalie Colloc'h

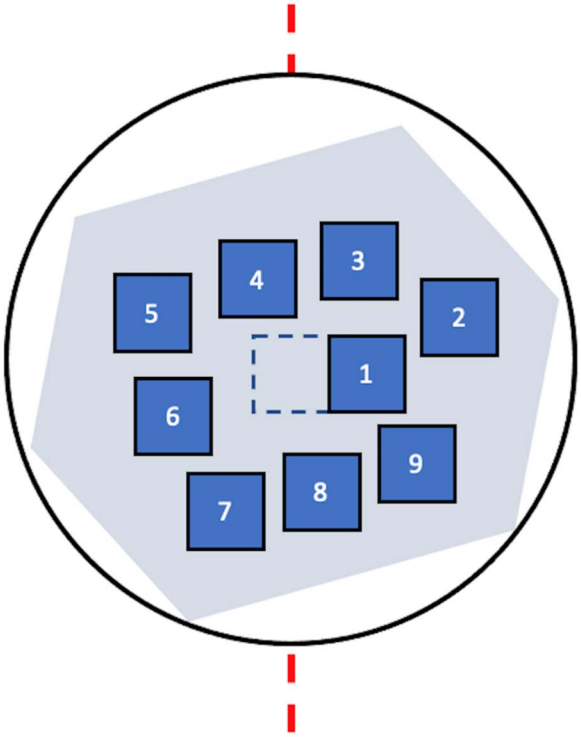

Figure S1 Schematic view of a crystal within the compression cavity of the DAC, showing the typical data collection strategy used on a large sample. The vertical rotation axis is indicated by the red dashed line. Prior to data collection, the cavity is centered using X-rays with a highly attenuated beam. The centering zone is indicated with a dashed square. Blue squares, representing a beam size of 50 µm × 50 µm, show the possible irradiation zones. We tried to exploit the zones close to the center when the DAC is rotated at the largest angles to avoid interaction of the beam with the metallic gasket. In the present study, the data set at 210 MPa was collected using the 3 zones 1-3, and the data set at 310 MPa using the 3 zones 5-7.

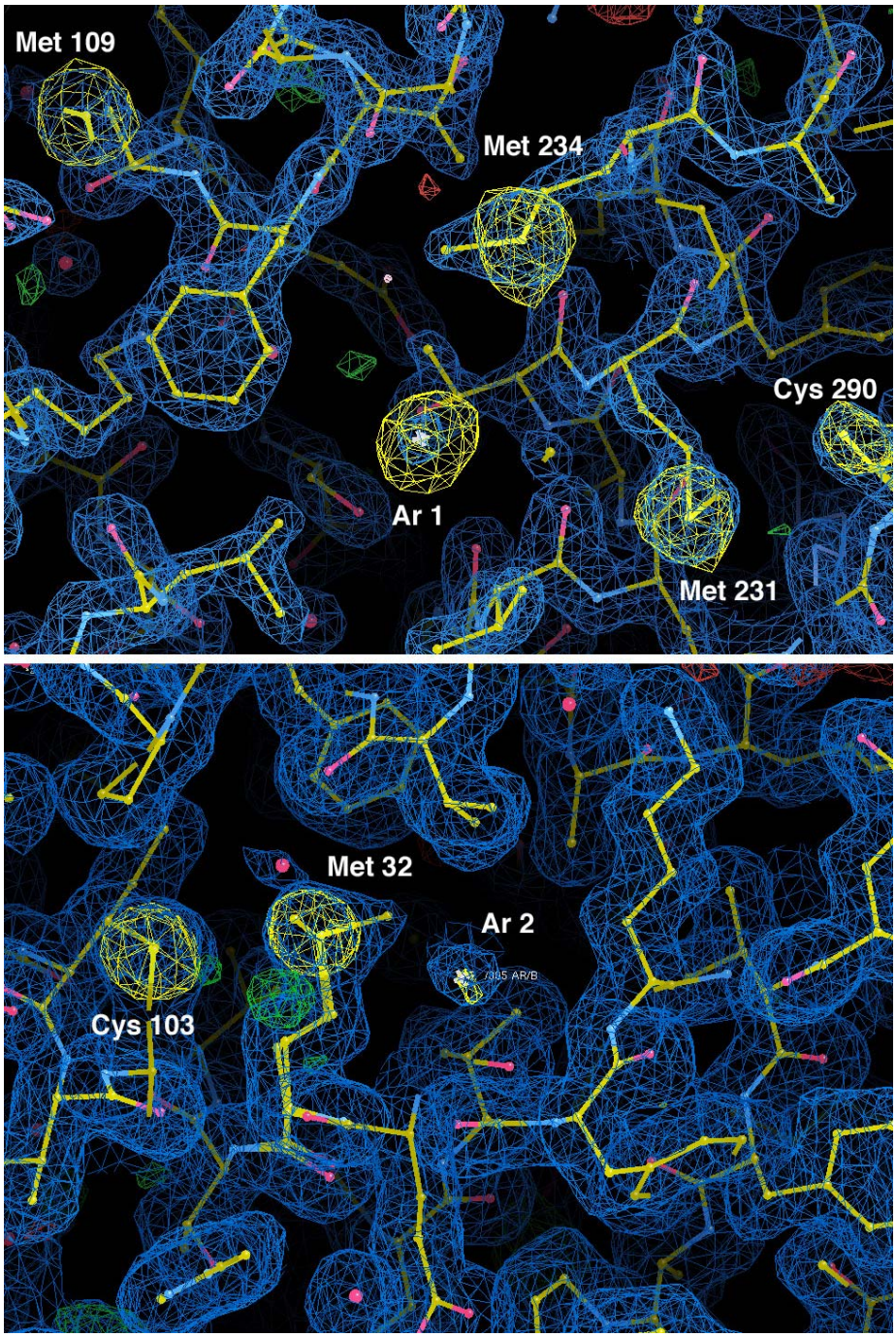

Figure S2 Anomalous map of UOX-HArP-60-T100 calculated using data collected at a wavelength of 1.7 Å (in yellow, contouring at 4σ) around the argon atom (Δf'' ~ 0.9 e^-) and the sulfur atom (Δf'' ~ 1.1 e^-) of a neighbouring methionine. Argon is bound in the main binding site (*upper*) close to Met 231 and in the minor binding site (*lower*) close to Met 32. The 2Fo-Fc map (contouring at 1.7σ) is in blue.

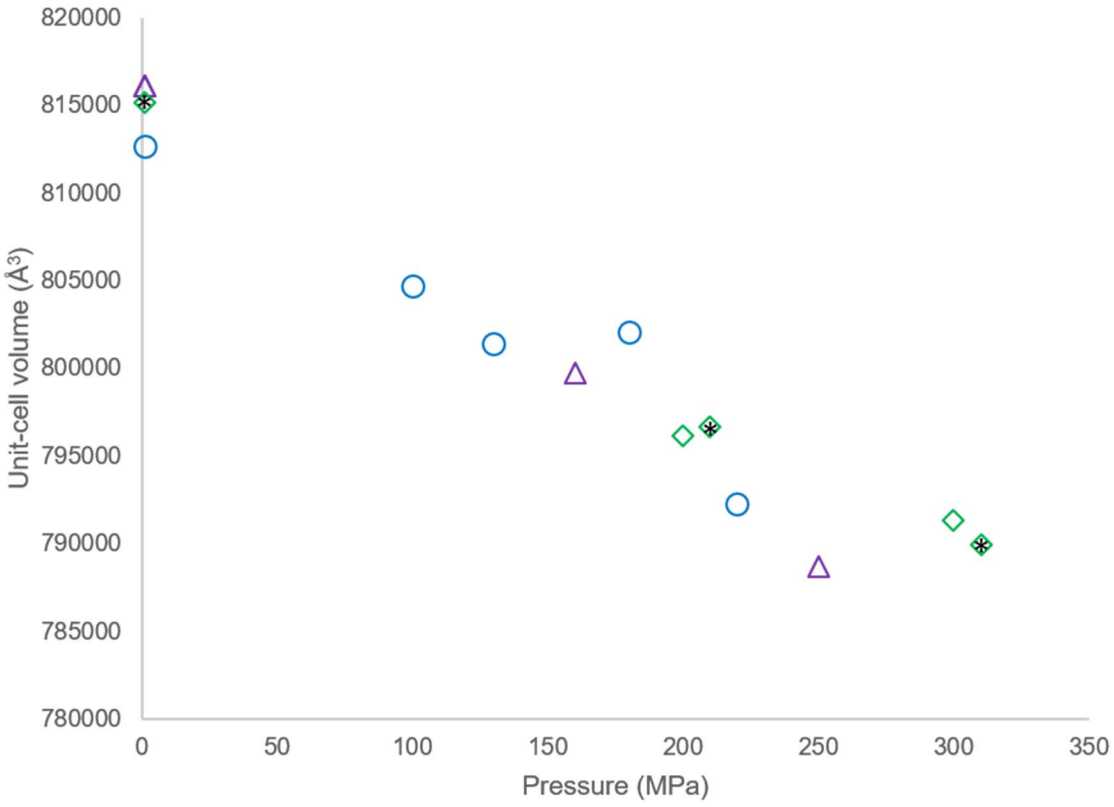

Figure S3 Compressibility curves showing the unit-cell volume which decreases linearly with pressure for three independent experiments at different synchrotrons: ID27 beamline in 2006 at ESRF (Grenoble, France) shown with blue circles, I19 beamline in 2019 at Diamond Light Source (Didcot, UK) shown with purple triangles and CRISTAL beamline in 2019 at SOLEIL (Gif sur Yvette, France) shown with green diamonds. The three full data collections described in the paper (UOX-HHP-0.1-RT, UOX-HHP-210-RT and UOX-HHP-310-RT) are shown with a star.

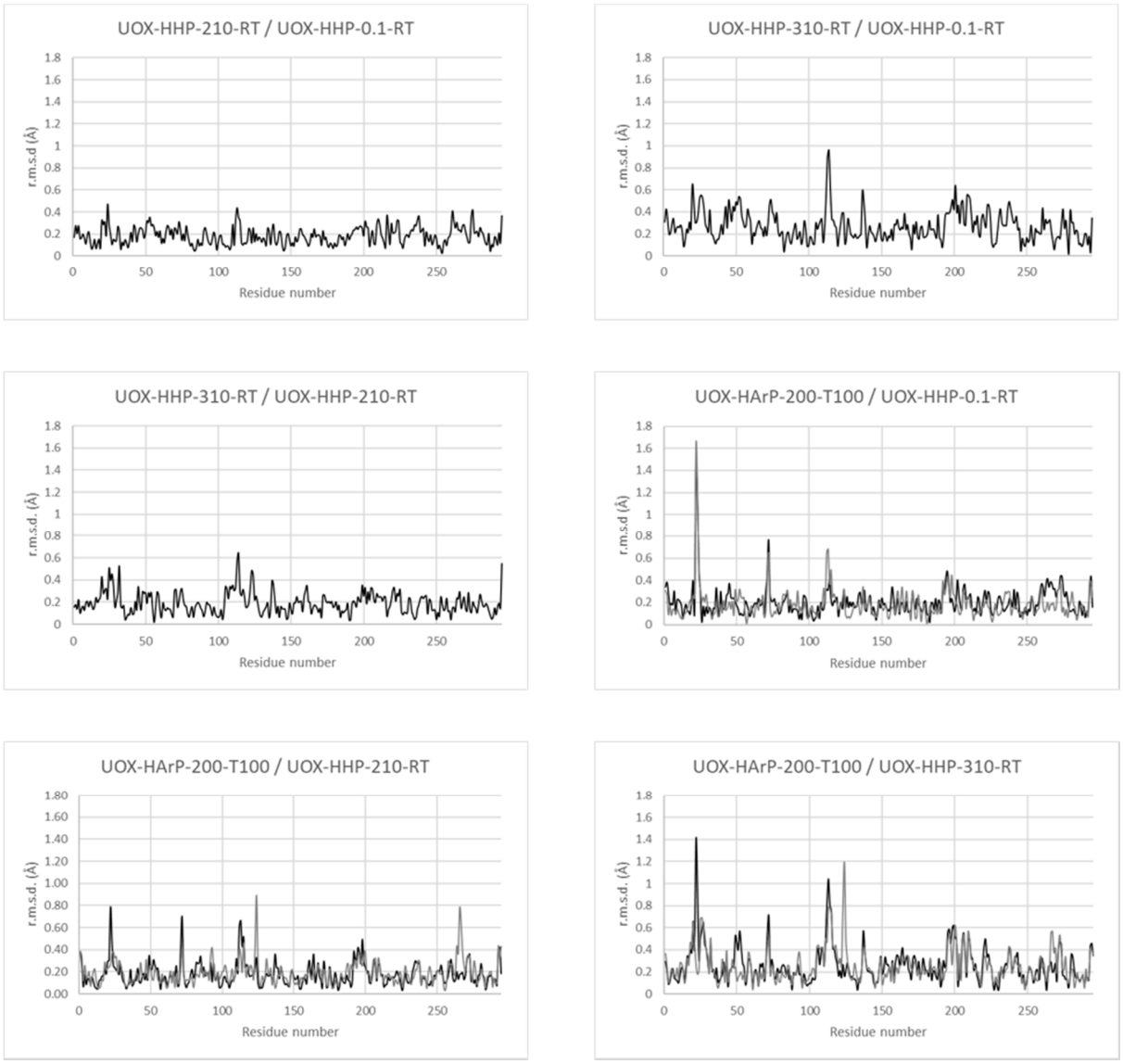

Figure S4 Cα r.s.m. deviations between the UOX-HHP-RT structures at three different pressures and between the UOX-HArP-200-T100 structure (A chain in black and B chain in grey) and the three UOX-HHP-RT structures.

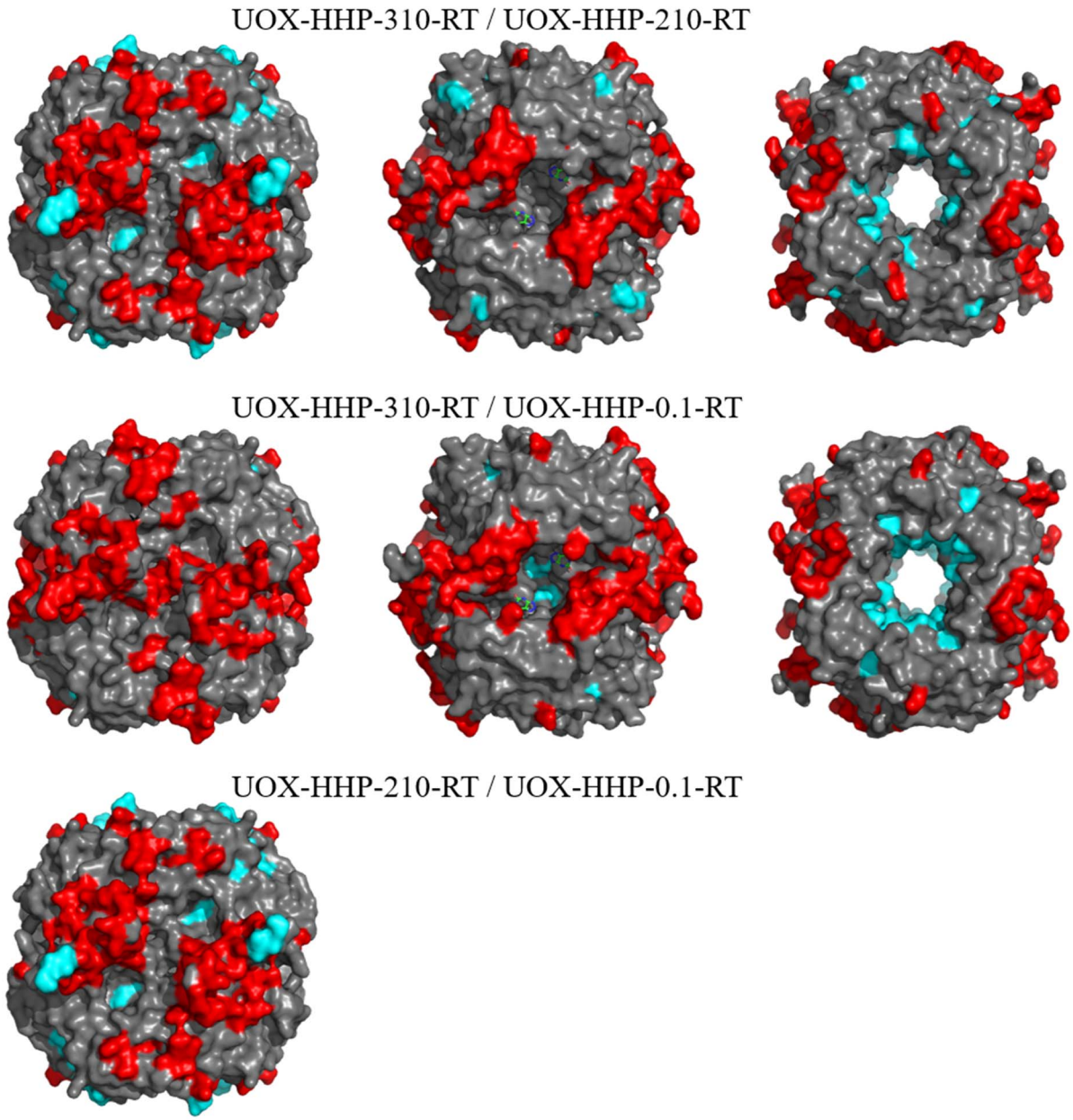

Figure S5 Molecular surface of the UOX tetramer, along the *a* axis (*left*), the *b* axis (*middle*) and the *c* axis (*right*). *Upper*: Comparison between UOX-HHP-310-RT and UOX-HHP-210-RT, with an average *B*-factor increase of 19 Å^2 ± 4.9 Å^2, coloured in red when the increase is higher than 24 Å^2, in cyan when the increase is lower than 14 Å^2, and in grey otherwise. *Middle*: Comparison between UOX-HHP-310-RT and UOX-HHP-01-RT, with an average *B*-factor increase of 28 Å^2 ± 7.3 Å^2, coloured in red when the increase is higher than 35 Å^2, in cyan when the increase is lower than 20 Å^2, and in grey otherwise. *Lower*: Comparison between UOX-HHP-210-RT and UOX-HHP-01-RT, with an average *B*-factor increase of 8.9 Å^2 ± 3.9 Å^2, coloured in red when the increase is higher than 13 Å^2, in cyan when the increase is lower than 5 Å^2, and in grey otherwise. The view along the *b* and *c* axes are shown in the lower part of Fig. 1.

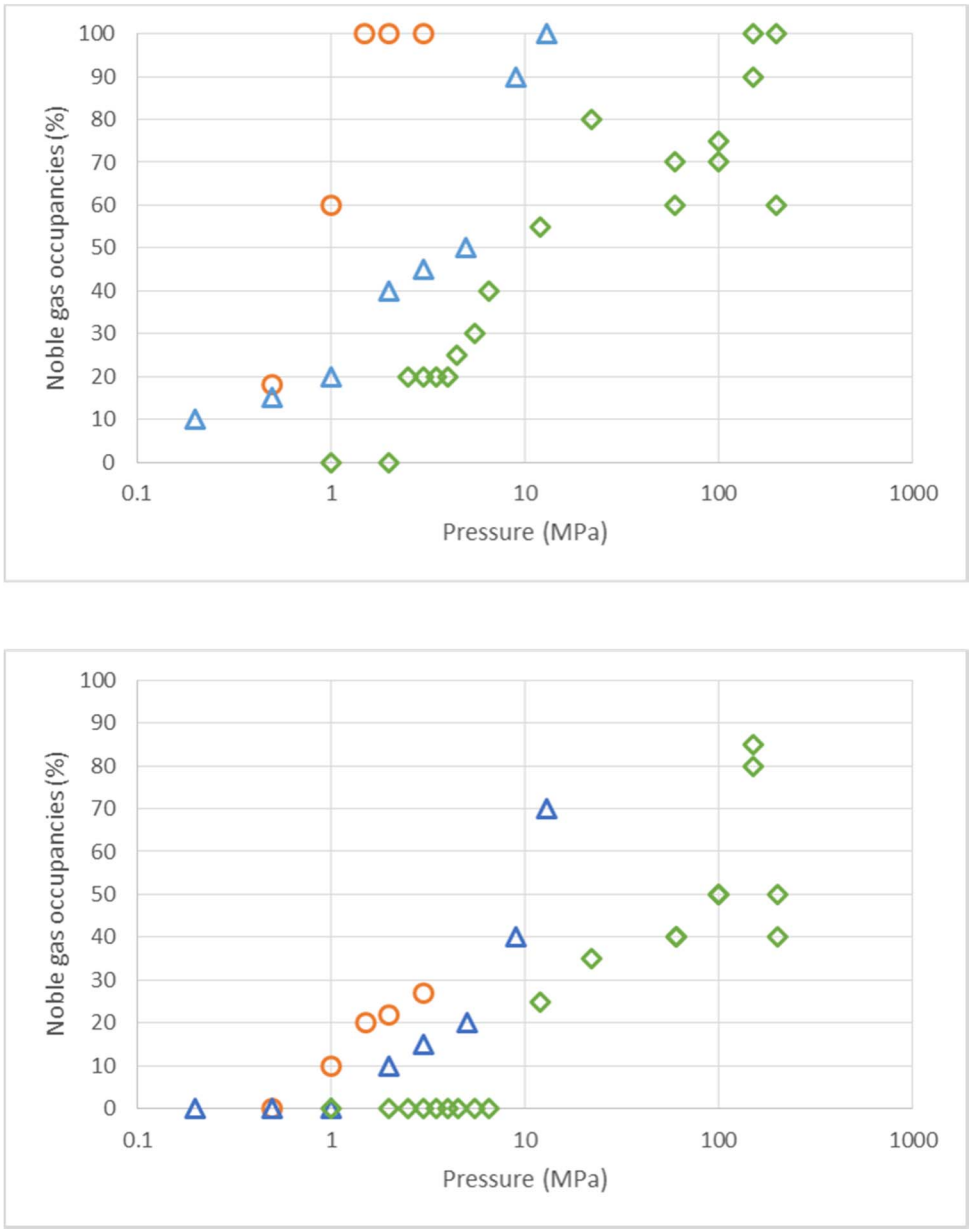

Figure S6 Occupancies for the three noble gases (xenon shown with orange circles, krypton with blue triangles and argon with green diamonds) as a function of the applied pressure in logarithmic representation for the main binding site in the cavity (*upper*) and in the minor binding site (*lower*). Data from (Marassio *et al.*, 2011; Colloc'h *et al.*, 2011), PDB entries *6ic1* and *6rgm* (unpublished data) and this manuscript.

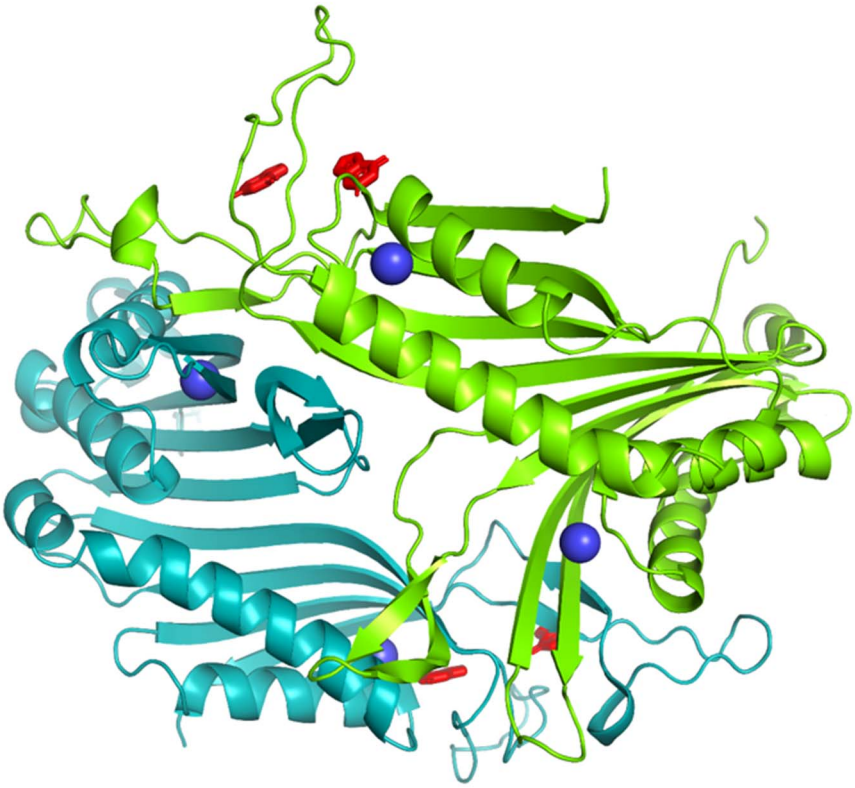

Figure S7 The two chains of UOX in the asymmetric unit of the UOX-HArP-200-T100 structure with the A chain in green, the B chain in cyan, the four Ar atoms as blue spheres and the four 8-azaxanthine molecules in red stick representation.